A SUPPLEMENTARY MATERIAL

A.1 Cell compartment pH

Table 1 lists the pH of all cellular compartments included in the human reconstruction. The three techniques used most frequently to study intracellular pH are pH-sensitive microelectrodes, pH-sensitive dyes and nuclear magnetic resonance. Imaging cells loaded with pH-sensitive dyes is the only method with enough spatial resolution to measure pH in individual organelles (1). The values in table 1 were all obtained in live mammalian cells using pH sensitive fluorescent dyes targeted to the desired cell compartment.

According to the Beer-Lambert law fluorescence depends not only on the extinction coefficient of the fluorescent molecule but also on its concentration and the length of the light's path through the sample. Both concentration and path length are impossible to measure in a cell. To factor out these variables researchers employ either dual emission or dual excitation ratiometric fluorescence methods. Either the excitation wavelength is held constant and emission recorded at two different wavelengths, or the sample is excited at two different wavelengths and emission is recorded at a single wavelength. Which method is used depends on the excitation and emission spectra of the particular fluorescent probe. By taking the ratio of light emission at two emission or excitation wavelengths, concentration and path length cancel out (1).

Factors that may influence the outcome of intracellular fluorescence pH measurements include cell type, choice of dye (2) and the method used for in vivo fluorescence calibration. The two calibration methods used most frequently are the nigericin method and the null method. The null method requires fewer assumptions about the intracellular environment (3). Preference was here placed on studies using human cells transfected with pH-sensitive mutants of green fluorescent protein where fluorescence was calibrated in vivo using the null method.

A.1.1 Cytosol and nucleus

Buckler and Vaughan-Jones were first to introduce the use of a new pH sensitive fluorescent probe, carboxy-SNARF-1 (pKa $\approx$ 7.5), for measurements of cytosolic pH (4). Previously, BCECF had been the most popular intracellular pH sensor. The main advantage of carboxy-SNARF-1 is that it is a dual emission fluorophore while BCECF is a dual excitation fluorophore. The two signals needed for ratiometric pH measurements can therefore be recorded simultaneously. Carboxy-SNARF-1 also has two pH sensitive emission peaks while BCECF has only one. Buckler and Vaughan-Jones loaded carboxy-SNARF-1 into cells by dissolving the acetoxymethyl ester of the dye in the cell medium. In this form the dye readily diffuses through the cell membrane into the cell where it is hydrolyzed by intracellular esterases. Once hydrolyzed it is retained within the cell. Buckler and Vaughan-Jones used the dye to measure cytosolic pH in type-1 cells from the carotid body of neonatal rats. When the dye was calibrated using the nigericin method they obtained a pH of 7.23 $\pm$ 0.04 and when calibrated using the null method the pH was 7.18 $\pm$ 0.05. Benink et al(5) were are able to detect a statistically significant difference between nuclear and cytoplasmic pH in U2OS cells, 7.43 $\pm$ 0.13 and 7.05 $\pm$ 0.08, respectively. They discuss that this "tends to differ with cell type" and the issue seems to still be a matter of debate so we assume the same pH for cytoplasmic and nuclear pH.

A.1.2 The endoplasmic reticulum, Golgi apparatus and lysosomes

Studies on the pH of organelles in the secretory and endocytic pathways were reviewed in Physiology in 2004 (6). It has been confirmed repeatedly that pH gradually decreases down the secretory pathway. The pH of the endoplasmic reticulum is around 7.2 or near neutral while the cis Golgi network is slightly acidic with a pH of approximately 6.7. There is a gradual drop in pH inside the Golgi apparatus moving towards the trans face and in the trans Golgi network the pH is around 6.0. In secretory granules the pH drops as low as 5.2. A pH gradient in the opposite direction has been observed in the endocytic pathway towards the lysosomes. While early endosomes are thought to have a pH of around 6.3, lysosomes are much more acidic with a pH of approximately 5.5.

A.1.3 Extracellular

Street et al. measured pH in the interstitial fluid of human skeletal muscle (7). Microdialysis dialysates of interstitial fluid were collected continuously from the quadriceps muscles of six healthy adult males at rest and during exercise. pH in the dialysates was measured using the pH sensitive probe BCECF. Mean interstitial pH at rest was 7.38 $\pm$ 0.02.

A.1.4 Mitochondria

Mitochondrial pH has been measured in HeLa cells (8, 9), neonatal rat cardiomyocytes (9) and in human umbilical vein endothelial cells (ECV304) (10). In all cases the pH was found to be close to 8.0.

Llopis et al. transfected HeLa cells and neonatal rat cardiomyocytes with the pH sensitive GFP mutant EYFP-mit (pKa = 6.4) (9). EYFP-mit was targeted to the mitochondrial matrix by fusing it with a short peptide from a mitochondria specific protein. The subcellular location of EYFP-mit was confirmed by co-staining cells with the traditional mitochondrial dye rhodamine 124. Fluorescence was calibrated in vivo using the nigericin method. Mitochondrial pH was found to be 7.98 ± 0.07 in HeLa cells and 7.91 ± 0.16 in cardiomyocytes. Using the same method Porcelli et al. measured a pH of 7.78 ± 0.17 in ECV304 cells (10).

Abad et al. repeated the experiment on HeLa cells using a different GFP mutant they called mtAlpHi (8). The pKa of mtAlpHi is around 8.5 which makes it more suitable than EYFP-mit as a pH indicator in basic solutions. Mitochondrial pH, when measured with mtAlpHi, was found to be 8.05 ± 0.11.

A.1.5 Peroxisomes

Peroxisomal pH has not been determined conclusively. Values ranging from 5.8-8.2 have been reported (11, 12, 13, 14, 15). Researchers are divided into two camps on the issue (16). One group maintains that the peroxisomal membrane is freely permeable to solutes and that the pH of the peroxisomal lumen is therefore the same as the cytosol's, or approximately neutral (13) . The other camp holds that the peroxisomal membrane is impermeable and that a proton gradient exists across it which is maintained by a proton pump. Within this camp there is still disagreement on whether protons are pumped into or out of the peroxisomes, and while some studies done in yeast have concluded that peroxisomes are acidic (12, 14), others done both in humans and in yeast reported a basic pH (11, 15).

Jankowski et al. put forth convincing evidence that the pH of peroxisomes was neutral (13). Peroxisomal pH was measured in Chinese hamster ovary (CHO) cells and human foreskin fibroblasts. CHO cells were transfected with pHluorin-SKL (pKa ≈ 6.5) while human foreskin fibroblast were transfected with eGFP-SKL (unspecified pKa). Both proteins are pH sensitive GFP mutants that have the peroxisomal targeting sequence SKL attached to their carboxyl terminal. The proteins were confirmed to be confined to peroxisomes by double-staining with catalase antibodies once pH measurements had been completed. When fluorescence was calibrated in vivo using the nigericin method the pH of CHO cell peroxisomes was found to be 7.12 ± 0.13 but when the null method was used for calibration the measured pH was 6.92 ± 0.04. Peroxisomal pH in human foreskin fibroblasts was measured at 7.17 ± 0.22 using the nigericin method for calibration. The authors attributed the difference in their results and those of earlier studies (11, 14) to methodological differences.

Later however van Roermund et al., using a very similar experimental design as Jankowski et al., reported peroxisomal pH to be 8.2 ± 0.2 in the yeast S. cerevisiae (15). Cells were transfected with a different pH sensitive GFP mutant, EYFP(H148G)-SKL that has pKa = 8.0. Roermund et al. claimed that the much lower pH obtained by Jankowski et al. was due to the fact that pHluorin's pKa is too low to reliably detect the high pH of peroxisomes.

Antonenkov and Hiltunen have suggested that peroxisomal pH may be variable and may depend on the physiological state of the cell (16). This suggestion was part of the reasoning behind a new theory they put forth on the permeability of the peroxisomal membrane. They had previously produced evidence that the membrane was permeable to small solutes up to 300 Da but not to cofactors and other larger solutes (17). According to their theory small solutes such as protons and hydroxide ions do diffuse freely through pores in the membrane but a pH gradient may still form across it if the distribution of charges in the peroxisomes and the cytosol is uneven i.e., a Donnan equilibrium may be reached (16, 18). Matrix proteins in mouse and rat liver peroxisomes are mainly positively charged, and thus are more likely to attract hydroxide ions and repel protons (18). The distribution of macromolecular charges between the peroxisomes and the cytosol is, however, not the only determinant of the Donnan potential across the peroxisomal membrane. Charges on other large solutes such as adenine nucleotides, that do not cross the membrane freely, also contribute to the equilibrium Donnan potential (18). This may explain the observed variability in peroxisomal pH.

A.2 Cell compartment electrical potential

Electrical potential differences across compartmental membranes affect the thermodynamics of ion transport between compartments. As metabolites transported into or out of cellular compartments usually pass through the cytosol we define the electrical potential across each compartment's membrane ($\Delta\phi_{compartment}$) relative to the cytosol so that $\Delta\phi_{compartment} = \phi_{compartment} - \phi_{cytosol}$. Membrane potentials in the eight compartments included in Recon

1 are listed in Table S1, and the relevant literature is reviewed in the following sections. As with pH we assume that no electrical potential difference exists between the cytosol and nucleus.

A.2.1 Mitochondria

Electrical potential differences across the inner mitochondrial membrane ($\Delta\phi_m$) have been measured in isolated mitochondria and in intact cells from various tissue (19). Values measured in intact cells have ranged from -80 to -160 mV depending on species, cell type and experimental design. Measurements in isolated mitochondria have generally yielded higher values ranging from -150 to -220 mV.

We chose to use measurements made in intact rat hepatocytes using the cationic fluorophore $TPMP^+$. Three similarly designed studies reported $\Delta\phi_m$ values of -155.2 ± 5.2 mV (20), -161 ± 2.6 mV (21) and -150 ± 1.0 mV (22). We used an intermediate value of -155 mV for $\Delta\phi_m$.

A.2.2 Extracellular fluid

It is well established that electrical potential differences across the plasma membrane ($\Delta\phi_e$) are cell type specific and that the difference is greatest in excitable cells (23). We chose to use the membrane potential of a nonexcitable cell type as most cells fall into that category. Hepatocytes were a convenient choice since two of the three papers cited above for mitochondrial membrane potential in rat hepatocytes also reported plasma membrane potentials in the same cells. The values reported for $\Delta\phi_e$ in the two papers were 32.8 ± 2.4 mV (21) and 27.8 ± 2.0 mV (22).

A.2.3 Golgi apparatus

The Golgi membrane potential ($\Delta\phi_g$) has not to our knowledge been measured directly. The membrane of the Golgi apparatus has been shown to contain an electrogenic, V-ATPase proton pump (24) but $\Delta\phi_g$ is nevertheless assumed to be negligible (25, 6, 26). The reason for this is the presence of large counterion (K^+, Cl^-) conductances through the Golgi membrane. After a comprehensive investigation of the factors that regulate Golgi pH, Schapiro et al. (25) concluded that the flux of counterions through the Golgi membrane was at least as high as influx of protons driven by the V-ATPase. Golgi membrane potential was therefore assumed to be small or nonexistent. They further concluded that Golgi pH was regulated by a balance between active transport of protons into the Golgi lumen by the V-ATPase and passive leak of protons or their equivalents (like OH^-) across the Golgi membrane.

A.2.4 Endoplasmic reticulum

The membrane of the endoplasmic reticulum (ER) does not contain active H^+ V-ATPase (26, 27) and it's permeability to proton equivalents is approximately three times greater than the Golgi membrane (26). Permeability of the ER membrane to the counterions K^+ and Cl^- is similar to that of the Golgi (26). These facts combined have lead researchers to conclude that the ER membrane potential is negligible (26, 27).

A.2.5 Lysosomes

A method for noninvasive measurement of lysosomal membrane potential, based on fluorescence resonance energy transfer (FRET), has recently been developed (28). Steady-state lysosomal membrane potential in mouse RAW264.7 macrophages averaged 19 mV. Evidence suggested that approximately half of this electrical potential was generated by the activity of H^+ V-ATPases in the lysosomal membrane, whereas the other half was generated by Donnan effects.

A.2.6 Peroxisomes

As discussed in Section A.1.5, current theories suggest that a variable pH gradient (ΔpH) may be generated across the peroxisomal membrane by a variable Donnan potential that depends on the distribution of large, charged solutes between the peroxisomes and cytosol (16, 18). The proton motive force $\Delta_r G'_p$ i.e., the transformed Gibbs energy for transport of a mole of protons across a semipermeable membrane, is obtained by rewriting Eq. 5 as

$$\Delta_r G'_p = -2.303 \times RT \times \Delta\mathrm{pH} + F \times \Delta\phi.$$

If an equilibrium ion distribution is reached, such that $\Delta_r G'_p = 0$, membrane potential is related to the pH gradient across the membrane by;

$$\Delta\phi = -\frac{2.303 \times RT \times \Delta\mathrm{pH}}{F}.$$

In peroxisomes where $-1.40 \leq \Delta\text{pH} \leq 1.00$ we therefore have that $-61.6\,\text{mV} \leq \Delta\phi \leq 86.2\,\text{mV}$.

A.3 Uncertainty in thermodynamic data

A.3.1 Uncertainty in standard transformed metabolite Gibbs energy of formation

Here we describe how we propagate uncertainty in experimental thermodynamic measurements or estimated thermodynamic parameters together with uncertainty arising from missing data, into our calculation of metabolite Gibbs energy of formation. Let $u^s_{f,i}$ denote uncertainty in $\Delta_f G'^0_{i,est}$, due to the standard error in Gibbs energy contribution estimates for structural groups. The Gibbs energy contribution of each group included in the group contribution method was reported with a standard error; $\mathbf{SE_{gr}} \in \mathbb{R}^{g,1}$ (29). We assume uncertainty is given by

$$u^s_{f,i} = 2 \times \sqrt{\sum_{p=1}^{g} \left(G_{i,p} \cdot SE_{gr,p}\right)^2}, \tag{11}$$

where $G_{i,p}$ is an element of a group enumeration matrix $\mathbf{G} \in \mathbb{N}^{m,g}$, and indicates the number of occurrences of the p^{th} group in the structure of the i^{th} metabolite. $SE_{gr,p}$ is the standard error for the p^{th} group. The group enumeration matrix $\mathbf{G}$, is constructed by von Bertalanffy 1.1 using the output from the group contribution software by Jankowski et al (29).

Let $u^a_{f,i}$ denote the uncertainty in measured metabolite Gibbs energy of formation $\Delta_{f,i} G^0_{obs}$. Although $u^a_{f,i}$ is not specified in Alberty's textbooks, we take it as 4 kJ/mol as experimental error is generally between 0.04-4 kJ/mol (29).

Let $u^p_{f,i}$ denote the uncertainty in $\Delta_f G'^0_{i,est}$ due to uncertainty in pK_a estimates of the metabolite species in the corresponding pseudoisomer group. By comparison with experimental measurements, Szegezdi et al. (30) deemed 0.75 to be the standard error in pK_a estimation by the ChemAxon plugin. This error was factored into uncertainty in $\Delta_f G'^0_{i,est}$ in proportion to the relative abundance of species other than the predominant species at pH 7. For example; a metabolite with a 0.7 mol fraction of the predominant species has $u^p_{f,i} = 2 \times RT \ln(10) \times (1 - 0.7) \times 0.75 = 1.16$ kJ/mol (see Eq. 3). $u^p_{f,i}$ would be at its maximum theoretical value of 8.56 kJ/mol for metabolites represented by nonpredominant species only. No Maximum $u^p_{f,i}$ for Recon 1 metabolites was 3.72 kJ/mol, as no metabolite was represented by nonpredominant species only.

Let $u^H_{f,i}$ denote the uncertainty due to our assumption that $\Delta_f H^0_j = \Delta_f G^0_j$ for metabolite species in pseudoisomer group i. As Alberty provides $\Delta_f H^0_{j,obs}$ for a subset of metabolite species we could calculate that 14.27 kJ/mol is the standard error in $\Delta_f G'^0_i$ associated with our assumption. We set the uncertainty for all metabolites at twice the standard error; $u^H_{f,i} = 2 \times 14.265 = 28.53$ kJ/mol. From the same subset of metabolite species, we could also calculate that 27.70 kJ/mol is the standard error in $\Delta_f G'^0_i$ if one does not make any adjustment for the difference between room temperature and body temperature, 298.15 and 310.15 K respectively. This demonstrates the importance of adjusting $\Delta_f G'^0_i$ for temperature even though comprehensive experimental data on standard enthalpies are still desirable.

Let $u^I_{f,i}$ denote the uncertainty associated with the absence of experimental data on ionic strength. We calculate the minimum and maximum $\Delta_f G'^0_i$ achievable with the assumption that ionic strength is between 0.05 and 0.25 M (31) and take $u^I_{f,i} = \frac{1}{2} \times \left(\max\left(\Delta_f G'^0_i(I)\right) - \min\left(\Delta_f G'^0_i(I)\right)\right)$. We find that $u^I_{f,i}$ was less than 8.75 kJ/mol for 95% of metabolites, and the maximum $u^I_{f,i}$ was 19.61 kJ/mol. The effect of ionic strength on $\Delta_f G'^0_i$ is greatest for metabolites that have a low charge relative to the number of hydrogen atoms or vice versa (see Eq. 2). Examples are acyl-CoAs, acyl-carnitines and starch.

Let $u^x_{f,i}$ denote uncertainty in $\Delta_f G'^0_i$ for peroxisomal metabolites due to variability in peroxisomal pH (see Table S1). We take $u^x_{f,i} = \frac{1}{2} \times \left(\max\left(\Delta_f G'^0_i(\text{p}H_x)\right) - \min\left(\Delta_f G'^0_i(\text{p}H_x)\right)\right)$ where pH_x is peroxisomal pH. $u^x_{f,i}$ was large for most of the 137 peroxisomal metabolites in Recon 1, and went as high as 584.40 kJ/mol.

Overall uncertainty in $\Delta_f G'^0_{i,est}$ was calculated as $u_{f,i} = \sqrt{\left(u^s_{f,i}\right)^2 + \left(u^p_{f,i}\right)^2 + \left(u^H_{f,i}\right)^2 + \left(u^I_{f,i}\right)^2 + \left(u^x_{f,i}\right)^2}$, and overall uncertainty in $\Delta_f G'^0_{i,obs}$ was $u_{f,i} = \sqrt{\left(u^a_{f,i}\right)^2 + \left(u^H_{f,i}\right)^2 + \left(u^I_{f,i}\right)^2 + \left(u^x_{f,i}\right)^2}$. As discussed in Section A.3.2 uncertainty in standard transformed reaction Gibbs energy is not the sum of uncertainty for each $\Delta_f G'^0_i$ involved in a reaction. However, quantification of uncertainty for individual metabolites is still necessary when reporting these values.

A.3.2 Uncertainty in standard transformed reaction Gibbs energy

As we use a group contribution method that linearly approximates the group contribution to standard Gibbs energy of formation, when calculating this uncertainty in reaction Gibbs energy, denoted$u^s_{r,k}$, one need only consider the groups that are either created or destroyed in the reaction. Therefore for the k^{th} reaction, which only involves metabolites with group contribution estimates we use

$$u^s_{r,k} = 2 \times \sqrt{\sum_{p=1}^{g} \left(\left(\mathbf{S}_k^T \cdot \mathbf{G}_p \right) \cdot SE_{gr,p} \right)^2}. \tag{12}$$

where $\mathbf{G}_p \in \mathbb{N}^{m,1}$ is the p^{th} column of the group enumeration matrix corresponding to the p^{th}group. As uncertainty in measured Gibbs energy is usually lower than uncertainty in estimated Gibbs energy (29), $u^s_{r,k}$ was also used as a slight overestimate of uncertainty in $\Delta_r G'^0_k$ due to uncertainty in $\Delta_f G^0_{j,obs}$.

Let $u^t_{r,k}$ denote the uncertainty in $\Delta_r G'^0_k$ due to the standard error in pK_a estimates and the assumption that $\Delta_f H^0_j = \Delta_f G^0_j$. We evaluated the actual $u^t_{r,k}$ using data for 150 reactions (34 nontransport reactions and 116 transport reactions), which only involved metabolites where both $\Delta_f G^0_{j,obs}$ and $\Delta_f H^0_{j,obs}$ were available in Alberty's tables. First; $\Delta_f G^0_j$ for all species of these metabolites, except the most basic species, were recalculated using estimated pK_a values in place of measured pK_a. With these $\Delta_f G^0_j$ the $\Delta_r G'^0_k$ for the aforementioned 150 reactions were calculated with $\Delta_f H^0_j$ set equal to $\Delta_f G^0_j$ for all species. With the $\Delta_r G'^0_k$ calculated in this manner, we took $u^t_{r,k}$ to be twice the standard error, which was 1.57 kJ/mol for nontransport reactions and 0.45 kJ/mol for transport reactions.

Let $u^I_{r,k}$ denote the uncertainty in $\Delta_r G'^0_k$ due to the assumption that compartmental ionic strength ranges from from 0.05 to 0.25 M. We calculated the minimum and maximum $\Delta_r G'^0_k$ achievable within this range and take $u^I_{r,k} = \frac{1}{2} \times \left(\max\left(\Delta_r G'^0_k\left(I\right) \right) - \min\left(\Delta_r G'^0_k\left(I\right) \right) \right)$. We found that $u^I_{r,k}$ was less than 1.87 kJ/mol for 95% of nontransport reactions, and less than 5.94 kJ/mol for 95% of transport reactions. Maximum $u^I_{r,k}$ was 8.65 kJ/mol for nontransport reactions and 23.80 kJ/mol for transport reactions.

Let $u^x_{r,k}$ denote uncertainty in $\Delta_r G'^0_k$ for peroxisomal reactions due to variability in peroxisomal pH and electrical potential (see Table S1). We take $u^x_{r,k} = \frac{1}{2} \times \left(\max\left(\Delta_r G'^0_k\left(\mathrm{p}H_x\right) \right) - \min\left(\Delta_r G'^0_k\left(\mathrm{p}H_x\right) \right) \right)$ where pH_x is peroxisomal pH. We found that $u^x_{r,k}$ was up to 11.30 kJ/mol for peroxisomal nontransport reactions, and up to 14.20 kJ/mol for peroxisomal transport reactions.

Overall uncertainty in $\Delta_r G'^0_k$ was calculated as $u_{r,k} \equiv \sqrt{\left(u^s_{r,k}\right)^2 + \left(u^t_{r,k}\right)^2 + \left(u^I_{r,k}\right)^2 + \left(u^x_{r,k}\right)^2}$ and used to define minimum and maximum standard transformed reaction Gibbs energy, $\Delta_r G'^0_{k,min} \equiv \Delta_r G'^0_k - u_{r,k}$ and $\Delta_r G'^0_{k,max} \equiv \Delta_r G'^0_k + u_{r,k}$ respectively.

A.4 Thermodynamic treatment of hydrogen ions and charge in multicompartmental metabolic reactions

Alberty (32, 31, 33) and more recently Jol et al. (34) derived relations which indicate how known constant hydrogen ion activity and electrostatic potential should be treated when there are one or more phases or compartments. We wish to add some clarity to those efforts by presenting a complementary derivation where the criterion for spontaneous change for a transport reaction is derived beginning with the first and second laws of thermodynamics and Gibbs' fundamental equation for the differential of internal energy. Jol et al. (34) arrive at the same end result, but start with the basic equation for the Gibbs energy of a mono-compartmental chemical reaction involving metabolite species, which is then supplemented with terms to model a multicompartmental chemical reaction involving reactants (representing pseudoisomer groups).

The second law of thermodynamics is a statistical law (35) which states that the entropy of an isolated system, which is of constant volume and is not in equilibrium, will tend to increase over time. At equilibrium, the entropy reaches a maximum (36). An isolated system is one with no material or energy exchange with the environment. In contrast, a living system is not an isolated system. However, the second law of thermodynamics can still be applied by considering a thought experiment in which a reaction is surrounded by a *bath* that maintains certain *intensive variables* constant (37). Together, the reaction and bath constitute a *thermodynamic system*. The value of an intensive variable, such as temperature, pressure, hydrogen ion activity or electrical potential, does not change if the size of the system under consideration changes. At typical laboratory conditions temperature is held constant using a heat bath, and the atmosphere acts as a bath to maintain a constant pressure. In biochemical thermodynamics the buffering capacity of intracellular proteins acts as a bath which maintains a constant hydrogen ion activity for each compartment. In a similar way, we can consider the electrical potential within a particular cellular compartment as a constant.

It is important to consider the definition of a thermodynamic system carefully. Most stoichiometric reconstructions are at the level of composite rather than elementary reactions, though there are exceptions (38). Within a composite metabolic reaction if one assumes each elementary reaction is thermodynamically feasible, then the composite reaction may be considered thermodynamically feasible. We shall consider each composite reaction and its bath as a thermodynamic system. Similarly, a single extreme pathway may be considered thermodynamically feasible if each composite reaction in that pathway is thermodynamically feasible, otherwise it is not thermodynamically feasible. However, since metabolic networks are composed of many extreme pathways with subsets of metabolites in common, it is an unsafe to speak about "thermodynamically feasible extreme pathways" (plural) unless one can confirm that reaction directionality assignments are globally thermodynamically consistent (39).

This paper is concerned with local thermodynamic feasibility considering *each* composite biochemical reaction and its own bath to be a *different* thermodynamically isolated system. A biochemical reaction can influence the bath either through a change in its volume, by heat exchange, by exchange of hydrogen ions or exchange of electrical charge. Because the entropy is a an *extensive variable*, the entropy of the combined system is the entropy of the metabolites in the reaction, $S_{metabolic}$, plus the entropy of the bath, S_{bath}. Likewise, the change in entropy of the combined system is the differential in entropy of the metabolites, $dS_{metabolic}$, plus the differential in entropy of the bath, dS_{bath}. By the second law of thermodynamics, the change in entropy over time, of the combined system, should be nonnegative

$$dS_{metabolic} + dS_{bath} \geq 0. \tag{13}$$

Away from equilibrium, this criterion for spontaneous change is a function of the change in entropy of the metabolites involved in the reaction and the change in entropy of the bath. However, we wish to derive a criterion for spontaneous change which is a function of the metabolites alone (36), so we aim to relate $d\mathrm{S}_{bath}$ to properties of the metabolites involved in the reaction.

According to Gibbs (40), the fundamental equation for the differential of internal energy of the bath is

$$dU_{bath} = TdS_{bath} - PdV_{bath} + \mu(H)dN(H)_{bath} + \mu(\phi)dQ_{bath} \tag{14}$$

where T is temperature, P is pressure and $\mu(H)$ is the hydrogen ion chemical potential (not including an electrical contribution to chemical potential) and $\mu(\phi)$ is the electrostatic contribution to the chemical potential for a charged species at a given electrostatic potential. Typically $\mu(\phi) = FQ\phi$, where F is Faraday's constant and Q is the charge of a species. These intensive variables are identically constant for the bath and the metabolites in the reaction. V_{bath} is the volume of the bath, $N(H)_{bath}$ is the number of hydrogen atoms in the bath and Q_{bath} is the number of electrical charges in the bath[1]. Observe that there is no change in abundance of any metabolite species in the bath other than hydrogen ions or charges.

[1]For present purposes we consider electrical charge as a species even though its "abundance" can be negative or positive.

Since the combined system and bath is isolated with respect to energy exchange with the environment, by the principle of conservation of energy, the differential in internal energy of the bath dU_{bath}, is equal and opposite to the differential in internal energy of the metabolite solution, $dU_{bath} = -dU_{metabolic}$. Likewise we assume that the total volume of the system plus the bath is constant, therefore we have $dV_{bath} = -dV_{metabolic}$. Similarly we assume that the total number of hydrogen ions in the system plus bath is constant, then by conservation of mass, we have $dN(H)_{bath} = -dN(H)_{metabolic}$. Finally we also assume that the total charge of the system and bath is constant so $dQ_{bath} = -dQ_{metabolic}$. These conservation relations follow as we consider the combined system to be thermodynamically isolated with respect to exchange of mass or energy with the environment.

If we substitute these conservation relations into (14), we have

$$dS_{bath} = \frac{-dU_{metabolic} - PdV_{metabolic} + \mu(H)dN(H)_{metabolic} + \mu(\phi)dQ_{metabolic}}{T} \tag{15}$$

and by substituting (15) for the dS_{bath} term in (13) we have

$$dU_{metabolic} + PdV_{metabolic} - TdS_{metabolic} - \mu(H)dN(H)_{metabolic} - \mu(\phi)dQ_{metabolic} \leq 0. \tag{16}$$

Note that the direction of the inequality is reversed at the same time as the signs have changed. Since we have a criterion for spontaneous change as a function of only metabolic terms, hereafter we omit the *metabolic* subscripts, as we manipulate (16) into a more useful form.

Let us define a thermodynamic potential, which we shall call the (Legendre) transformed Gibbs energy G', as

$$G' \equiv U + PV - TS - \mu(H)N(H) - \mu(\phi)Q \tag{17}$$

where the rationale for this particular definition will follow later. Since the transformed Gibbs energy of the metabolic system is a state variable, its exact differential (36) is

$$dG' = dU + PdV + VdP - TdS - SdT - N(H)d\mu(H) - \mu(H)dN(H) - Qd\mu(\phi) - \mu(\phi)dQ. \tag{18}$$

The net change in number of hydrogen ion*s* due to a reaction is

$$dN(H) = \sum_{j=1}^{N} N_j(H)dn_j, \tag{19}$$

where $N_j(H)$ is the number of hydrogen atoms in metabolite species j, n_j is the amount of species j, and N is the number of species in the system. The net change in charge due to a reaction is

$$dQ = \sum_{j=1}^{N} Q_j dn_j, \tag{20}$$

where Q_j is the charge of metabolite species j. The fundamental equation for the differential of internal energy for the N metabolite species in the reaction is

$$dU = TdS - PdV + \sum_{j=1}^{N} \mu_j dn_j, \tag{21}$$

where μ_j denotes the chemical potential of metabolite species j. Insertion of (19), (20) and (21) into (18) gives

$$dG' = VdP - SdT - N(H)d\mu(H) - Qd\mu(\phi) + \sum_{j=1}^{N} (\mu_j - \mu(H)N_j(H) - \mu(\phi)Q_j)dn_j. \tag{22}$$

This is a criterion for spontaneous change expressed in terms of change in pressure, temperature, hydrogen ion chemical potential, electrical potential and the abundance of each metabolite. If we define the Legendre transformed chemical potential of a metabolite species as the partial derivative of the transformed Gibbs energy

$$\mu'_j \equiv \left(\frac{\partial G'}{\partial n_j}\right) = \mu_j - N_j(H)\mu(H) - \mu(\phi)Q_j, \tag{23}$$

then for reactions which occur within a single compartment at constant pressure, temperature, hydrogen ion chemical potential and electrical potential, the criterion for spontaneous change is simply

$$(dG')_{P,T,\mu(H),\mu(\phi)} = \sum_{j=1}^{N} \mu'_j dn_j.$$

However, when a reaction involves transport of metabolite species between different compartments with possibly different hydrogen ion activity or electrical potential then the criterion for spontaneous change for a reaction is

$$(dG')_{P,T} = -N(H)d\mu(H) - Qd\mu(\phi) + \sum_{j=1}^{N} \mu'_j dn_j, \tag{24}$$

where $N(H)$ the net number of hydrogen ions transported from initial to final compartment, $d\mu(H)$ is the difference between initial and final compartment hydrogen ion chemical potential, Q is the net number of charges transported from initial to final compartment and $d\mu(\phi)$ is the difference between the appropriately scaled electrostatic potential between the initial and final compartment. Finally, note that the definition of the transformed Gibbs energy (17) was not chosen arbitrarily as the TdS and PdV in (18) have been canceled out by (18) and do not appear in (22). In addition the $\mu(H)dN(H)$ term for hydrogen ions and the $\mu(\phi)dQ$ terms for the charge in (18) have also been canceled out.

In accordance with Alberty (41), where there are reactions involving electric potential differences, the activity a_j of an ion can be defined in terms of its chemical potential μ_j; and the electric potential ϕ_k of the k^{th} compartment with

$$\mu_j = \mu_j^\circ + RT\ln(a_j) + FQ_j\phi_k.$$

In treating the fundamental equations of thermodynamics, chemical potentials of species are always used, but in making calculations when temperature and pressure are constant, chemical potentials are replaced by Gibbs energies of formation

$$\begin{aligned} \mu_j^\circ &= \Delta_f G_j^\circ \\ \mu_j &= \Delta_f G_j = \Delta_f G_j^\circ + RT\ln(a_j) + FQ_j\phi_k \end{aligned}$$

and Legendre transformed chemical potentials are replaced by transformed Gibbs energies

$$\begin{aligned} \mu_j^{\circ\prime} &= \Delta_f G_j^{\circ\prime} \\ \mu'_j &= \Delta_f G'_j \\ &= \Delta_f G_j - N_j(H)\Delta_f G(H_k) - FQ_j\phi_k \\ &= (\Delta_f G_j^\circ + RT\ln(a_j) + FQ_j\phi_k) - N_j(H)\Delta_f G(H_k) - FQ_j\phi_k \\ &= \Delta_f G_j^{\circ\prime} + RT\ln(a_j) \end{aligned}$$

where $\Delta_f G(H_k)$ denotes the Gibbs energy of formation of a hydrogen ion in compartment k. A consequence is that the Legendre transformed chemical potential of a hydrogen ion is zero in every compartment, irrespective of hydrogen ion activity or electrical potential. However, the direction of free diffusion of a hydrogen ion between two compartments with identical hydrogen ion activity, but different electrical potential, is determined by the sign of the driving force $(dG')_{P,T,\mu(H)} = -Qd\mu(\phi) = -d\mu(\phi)$, from (24), due to the transport of a positive charge between compartments.

Acid dissociation reactions equilibrate more rapidly than enzyme-catalyzed reactions. At the time scale of enzyme-catalyzed reactions, acid dissociation reactions can therefore be assumed to be at equilibrium. Because the transformed chemical potential of the hydrogen ion is always zero, chemical species that are related by acid dissociation reactions (acid-base pairs) have the same transformed chemical potential at the time scale of enzyme-catalyzed reactions. Chemical species that are related by acid dissociation reactions are known as pseudoisomer in analogy to structural isomers which have the same chemical potential at equilibrium (41). Because they have the same transformed chemical potential, terms for pseudoisomers in the summation in Eq. 24 can be collected to give

$$(dG')_{P,T} = -N(H)d\mu(H) - Qd\mu(\phi) + \sum_{i=1}^{N'} \mu'_i dn'_i, \tag{25}$$

where μ'_i is the transformed chemical potential of *pseudoisomer group* i, $n'_i = \sum n_j$ is the amount of pseudoisomer group i, and N' is the number of pseudoisomer groups in the system. In contrast to *chemical reactions*, which are treated in terms of individual chemical species, *biochemical reactions* are treated in terms of pseudoisomer groups.

Changes in the amounts of pseudoisomer groups in a system where a biochemical reaction occurs, are not independent but related through the reaction stoichiometry. The amount n'_i of pseudoisomer group i at any point in the biochemical reaction is (41);

$$n'_i = (n'_i)_0 + v'_i \xi', \tag{26}$$

where $(n'_i)_0$ is the initial amount of the pseudoisomer group in the system, v'_i is the stoichiometric coefficient for the pseudoisomer group in the reaction, and ξ' is the apparent extent of the reaction. The differential of n_i is then;

$$dn'_i = v'_i d\xi'. \tag{27}$$

Substitution of Eq. 27 into Eq. 25 gives;

$$(dG')_{P,T} = -N(H)d\mu(H) - Qd\mu(\phi) + \left(\sum_{i=1}^{N'} v'_i \mu'_i\right) d\xi'. \tag{28}$$

The *transformed reaction Gibbs energy* $\Delta_r G'$ of a reaction is defined as the rate of change of G' with the apparent extent of the biochemical reaction;

$$\Delta_r G' = \left(\frac{\delta G'}{\delta \xi'}\right)_{T,P} = -N(H)d\mu(H) - Qd\mu(\phi) + \sum_{i=1}^{N'} v'_i \mu'_i. \tag{29}$$

A.5 Concentrations of water and dissolved gases

In the treatment of biochemical reactions it is typical to assume an activity of water equal to one (42). In addition, we use the dissolved oxygen (reactant) concentration range, $0.1 - 8.6 \times 10^{-6}$ M . In aqueous phase the reactant carbon dioxide is distributed between a number of metabolite species, some involving water $[CO_2] = [CO_2(aq)] + [CO_3^{2-}] + [HCO_3^-] + [H_2CO_3]$. We assumed a carbon dioxide concentration of $[CO_2] = 1$ mM (43). The details follow the special thermodynamic treatment of carbon dioxide as described by Alberty, (Section 8.7 in (31)).

A.6 Reactions with inconsistent qualitative and quantitative directionality assignments

In Sections A.6.1 and A.6.2 we discuss our results for 19 reactions that had inconsistent qualitative and quantitative directionality assignments. All reactions are written out as they were in Recon 1 but with reaction arrows indicating their quantitative directionality.

A.6.1 Reactions with incorrect quantitative directionality assignments

Complex structural transformations The group contribution method used here does not appear to be suitable for estimation of reaction Gibbs energies for complex structural transformations such as opening or closing of rings. Four such reactions had conflicting qualitative and quantitative directionality. One of the four reactions was the final step in IMP synthesis;

$$\text{IMP} + H_2O \rightarrow \text{5-formamido-1-(5-phospho-D-ribosyl)imidazole-4-carboxamide},$$

which is catalyzed by IMP cyclohydrolase (E.C. 3.5.4.10). Kinetic studies on IMP cyclohydrolase have shown that this reaction is irreversible in the reverse direction (44). We estimated that $\Delta_r G'^0_k = -51.9 \pm 19.5$ kJ/mol and $\Delta_r G'_{k,max} = -2.6$ kJ/mol for the reaction so it was quantitatively irreversible in the forward direction. We attribute the incorrect quantitative directionality assignment to the complexity of the structural transformation that takes place in the reaction (Fig. S10a).

The other three ring opening or closing reactions that had conflicting qualitative and quantitative directionality included a nonenzymatic reaction from lysine degradation;

$$\text{1-piperideine-6-carboxylate} + H_2O + H^+ \leftarrow \text{L-allysine},$$

a similar nonenzymatic reaction from arginine and proline metabolism;

$$\text{L-glutamic 5-semialdehyde} \rightarrow \text{1-pyrroline-5-carboxylate} + H_2O + H^+,$$

and the photolysis of 7-dehydrocholesterol in skin;

$$7-\text{dehydrocholesterol} \leftarrow \text{previtamin D}_3.$$

An additional source of error in the standard transformed Gibbs energy estimate for the last reaction is that it is driven by UV radiation (45, 46) which was not considered in our thermodynamic calculations.

Photolysis of 7-dehydrocholesterol in skin is followed by spontaneous isomerisation of previtamin D_3 to vitamin D_3 (45, 46) in the reaction

$$\text{previtamin D}_3 \leftarrow \text{vitamin D}_3.$$

This is another complex structural transformation in the sense that previtamin D_3 is composed of a very different set of groups recognized by the group contribution method than vitamin D_3 (Fig. S10b). The equilibrium constant for the isomerisation at 37°C has been measured as 1.76 or 6.22 depending on the media (46), meaning $\Delta_r G'^0_k$ for the reaction is -1.4 or -4.7 kJ/mol. The reaction should therefore be reversible at intracellular conditions. We obtained $\Delta_r G'^0_k = 278.0 \pm 54.7$ kJ/mol and $\Delta_r G'_{k,min} = 193.5$ kJ/mol indicating that previtamin D_3 formation was highly favored. The group contribution method therefore appears to be unsuitable for estimation of the Gibbs energy for this reaction.

A.6.2 Reactions with correct quantitative directionality assignments

ATP-dependent excretion of bilirubin monoglucuronide into serum Bilirubin is a product of heme catabolism. Due to its hydrophobic nature it is transported in blood in complex with serum albumin. Under normal conditions it is taken up by hepatocytes where it is conjugated with glucuronide and secreted in bile (47). Under cholestatic conditions, where bile flow is hindered, bilirubin glucuronides (bilglcur) are excreted from hepatocytes into serum in an ATP dependent transport process;

$$\text{cytosolic bilglcur} + ATP + H_2O \rightarrow \text{extracellular bilglcur} + ADP + P_i + H^+.$$

This transport appears to be mediated by multidrug resistant protein 3 (MRPs) which is a member of the ATP binding cassette (ABC) family of transporters (48). ATP-dependent excretion of bilirubin glucuronide was qualitatively reversible but quantitatively forward with $\Delta_r G'_{k,max} = -20.3$ kJ/mol. The only metabolite in this reaction that had group contribution estimated $\Delta_f G^0_i$ was bilirubin glucuronide. As this metabolite appears on both sides of the reaction, our confidence in the $\Delta_r G'^0_k$ estimate is high.

Oxidation of L-4-Hydroxyglutamic semialdehyde An intermediate step in the metabolism of trans-4-hydroxy-L-proline to pyruvate and glyoxylate, is the oxidation of L-4-hydroxyglutamic semialdehyde by NAD to form erythro-4-hydroxy-L-glutamate;

$$\text{L-4-hydroxyglutamic semialdehyde} + NAD + H_2O \rightarrow \text{erythro-4-hydroxy-L-glutamate} + NADH + 2\,H^+.$$

This reaction was included in Recon 1 based on data in the KEGG database (49). It was qualitatively reversible but quantitatively forward with $\Delta_r G'_{k,max} = -17.6$ kJ/mol. The reaction is analogous to an intermediate step in the metabolism of proline to glutamate, which proceeds via an L-glutamic 5-semialdehyde intermediate (50, 51);

$$\text{L-glutamic 5-semialdehyde} + NAD + H_2O \rightarrow \text{glutamate} + NADH + 2\,H^+.$$

Both reactions are catalyzed by 1-pyrroline-5-carboxylate dehydrogenase (E.C. 1.5.1.12) in Recon 1. Oxidation of L-glutamic 5-semialdehyde is known to be irreversible (50, 51), which supports our results for oxidation of L-4-hydroxyglutamic semialdehyde.

Hydrolysis of S-formylglutathione Formaldehyde from exogenous and endogenous sources is detoxified in human cells through the combined action of formaldehyde dehydrogenase (E.C. 1.2.1.1) and S-formylglutathione hydrolase (E.C. 3.1.2.12). Formaldehyde dehydrogenase catalyses oxidation of formaldehyde in the reversible reaction (52)

$$\text{formaldehyde} + \text{reduced glutathione} + NAD \rightleftarrows \text{S-formylglutathione} + NADH + H^+.$$

S-Formylglutathione is then hydrolyzed by S-formylglutathione hydrolase in the reaction (53)

$$\text{S-formylglutathione} + H_2O \rightarrow \text{formate} + \text{reduced glutathione} + H^+.$$

The S-formylglutathione hydrolase reaction was qualitatively reversible but quantitatively forward with $\Delta_r G'_{k,max} = -7.6$ kJ/mol. Experiments have shown that the reaction is irreversible in the forward direction (53), supporting the quantitative directionality assignment.

Cytosolic and extracellular oxidation of glutathione Glutathione is vital to a variety of cellular functions. It reacts with free radicals to form less reactive chemicals, it is a substrate for several metabolic reactions, and it participates in regulation of multiple cellular processes (54). Glutathione is synthesized from glutamate, cysteine and glycine in two sequential reactions catalyzed by γ-glutamylcysteine synthetase (E.C. 6.3.2.2) and glutathione synthetase (E.C. 6.3.2.3) (54). In the cytosol and extracellular fluid, glutathione is oxidized to glutathione disulfide in the reaction

$$2\,\text{glutathione} + H_2O_2 \rightarrow \text{glutathione disulfide} + 2\,H_2O,$$

which is catalyzed by glutathione peroxidase (E.C. 1.11.1.9). Reduction of glutathione disulfide to glutathione is catalyzed by the NADPH-dependent glutathione reductase (E.C. 1.8.1.7) (54). The glutathione-glutathione disulfide couple is the most abundant redox couple in the cell and the glutathione:glutathione sulfide concentration ratio is often used as a measure of the cellular redox state (54, 55). This concentration ratio is high (>10) at normal conditions but is lowered when the cell is exposed to oxidative stress.

An experimentally determined equilibrium constant for the glutathione peroxidase reactions could not be found in the literature. The reactions were set to reversible in Recon 1 but we obtained $\Delta_r G'_{k,max} = -154.0$ kJ/mol for the cytosolic reaction and $\Delta_r G'_{k,max} = -151.7$ kJ/mol for the extracellular reaction, indicating that both reactions were irreversible in the forward direction. Our confidence in $\Delta_r G'^0_k$ for the reactions are high as they were determined using only $\Delta_f G'^0_{i,obs}$. Quantitative directionality is therefore most likely correct for these reactions.

Vitamin B6 metabolism Vitamin B6 is an essential nutrient for humans which occurs in diet as three distinct vitamers; pyridoxine, pyridoxamine and pyridoxal. The three vitamers differ only in the functional group present in the 4' position of the pyridine ring common to all of them. This position holds an aldehyde group in pyridoxal, an alcohol in pyridoxine and an amine in pyridoxamine (56, 57, 58). Inside cells, the three dietary vitamers are converted to pyridoxal 5'-phosphate; the main active form of vitamin B6. The first step in this conversion is phosphorylation of the pyridine ring in the 5' position by pyridoxal kinase (E.C. 2.7.1.35). This single step is sufficient to convert pyridoxal to pyridoxal 5'-phosphate but an additional oxidation step, catalyzed by pyridox(am)ine-5'-phosphate oxidase (E.C. 1.4.3.5) is required for complete conversion of the other two vitamers (56, 57, 58). The two pyridox(am)ine-5'-phosphate oxidase reactions are;

$$\text{pyridoxine 5'-phosphate} + O_2 \rightarrow \text{pyridoxal 5'-phosphate} + H_2O_2,$$

and

$$\text{pyridoxamine 5'-phosphate} + H_2O + O_2 \rightarrow \text{pyridoxal 5'-phosphate} + NH_4^+ + H_2O_2.$$

Both reactions were set to reversible in Recon 1. We obtained $\Delta_r G'_{k,max} = -53.6$ kJ/mol for the pyridoxine reaction and $\Delta_r G'_{k,max} = -59.6$ kJ/mol for the pyridoxamine reaction, so they were quantitatively forward. To our knowledge, the equilibrium constants of these reactions have not been measured but a different amine oxidase reaction has been shown to have a negative $\Delta_r G'^0_k$ of -19 kJ/mol (59). The functionality of Recon 1 was not affected by setting these reactions to irreversible in the forward directions. These facts combined lead us to conclude that the quantitative directionalities of these two reactions were correct.

Vitamin A metabolism Active forms of vitamin A in humans include the all-trans- and 13-cis-retinoic acid isomers (60). Each is formed by oxidation of the corresponding retinal isomer in a reaction of the type

$$\text{retinal} + \text{NAD(P)} + H_2O \rightarrow \text{retinoic acid} + \text{NAD(P)H} + 2\,H^+.$$

Oxidation of retinal isomers is catalyzed by retinal dehydrogenase (E.C. 1.2.1.36) (61). NAD-dependent oxidation of both all-trans- and 13-cis-retinal was qualitatively reversible but quantitatively forward with $\Delta_r G'_{k,max} = -7.2$ kJ/mol. Experiments with retinal dehydrogenase have shown that oxidation of retinal is irreversible (61) in agreement with the quantitative directionality assignment.

A.6.3 Reactions with potentially incorrect stoichiometries in Recon 1

Transport of negatively charged anions into the mitochondria Transport of coenzyme A, hydroxymethylglutaryl-CoA, octanoyl-CoA and carbonic acid between the cytosol and mitochondria was in each case modeled as reversible passive diffusion in Recon 1. As all four metabolites are negatively charged at physiological pH their transport into the mitochondria, against a negative membrane potential, is endergonic. All four passive diffusion reactions therefore had a positive standard transformed Gibbs energies and were quantitatively irreversible in the direction of transport out of the mitochondria. Unless the mitochondrial:cytosolic concentration gradients for these metabolites is that much higher, it is unlikely that they are transported into the mitochondria by passive diffusion.

Coenzyme A is known to be synthesized in the cytosol and transported into the mitochondria where it is used as a cofactor in the TCA cycle and β-oxidation of fatty acids (62). When Recon 1 was published the exact transport mechanism for coenzyme A was not known. Since then, a novel member of the mitochondrial carrier family has been discovered which was shown to transport coenzyme A by a counterexchange mechanism (63). The most likely candidates for exchange with coenzyme A were thought to be intramitochondrial adenine nucleotides, deoxy adenine nucleotides and adenosine 3',5'-diphosphate.

Formation of adenosine 5'-phosphosulfate (APS) 3'-Phosphoadenylyl sulfate (PAPS) serves as the sulfonate donor in all sulfotransferase reactions in humans (64). It is formed from inorganic sulfate and ATP in a two step process. In the first step, which is catalyzed by sulfate adenylyltransferase (E.C. 2.7.7.4) (64), inorganic sulfate reacts with ATP to form adenosine 5'-phosphosulfate;

$$\mathrm{ATP} + \mathrm{SO_4^{2-}} + \mathrm{H^+} \leftarrow \mathrm{APS} + \mathrm{PP}_i.$$

In the second step, catalyzed by adenylyl-sulfate kinase (E.C. 2.7.1.25) (64), APS combines with a second molecule of ATP to form PAPS;

$$\mathrm{APS} + \mathrm{ATP} \rightarrow \mathrm{PAPS} + \mathrm{ADP} + \mathrm{H^+}.$$

The adenylyl-sulfate kinase reaction was both qualitatively and quantitatively forward, whereas the sulfate adenylyltransferase reaction was qualitatively forward but quantitatively reverse with $\Delta_r G'_{k,min} = 7.3$ kJ/mol. Measurements of the apparent equilibrium constant for the sulfate adenylyltransferase reaction have ranged from 6.2×10^{-9} to approximately 1.1×10^{-8} (65, 66, 67, 68). The measured equilibrium constants correspond to $\Delta_r G'^0_k$ between 47.2 and 47.6 kJ/mol which agrees well with our $\Delta_r G'^0_k$ estimate of 48.3 ± 9.1 kJ/mol. The quantitative directionality assignment for the sulfate adenylyltransferase reaction was therefore correct.

Correcting the directionality of the sulfate adenylyltransferase reaction in Recon 1 would make the model incapable of producing PAPS. The reaction is driven in the forward direction in vivo by hydrolysis of pyrophosphate by inorganic diphosphatase (E.C. 3.6.1.1) (64). The overall reaction for APS formation is therefore;

$$\mathrm{ATP} + \mathrm{SO_4^{2-}} + \mathrm{H_2O} \rightleftarrows \mathrm{APS} + 2\,\mathrm{P}_i.$$

This reaction is quantitatively reversible with $\Delta_r G'^0_k = 23.9 \pm 11.9$ kJ/mol, $\Delta_r G'_{k,min} = -39.6$ kJ/mol, and $\Delta_r G'_{k,max} = 56.6$ kJ/mol. To correct the directionality assignment for the sulfate adenylyltransferase reaction in Recon 1, while still maintaining the capability of the model to produce PAPS, the first step of PAPS synthesis should be represented by the overall reaction.

A.7 Supplementary tables

Table S1: pH and electrical potential ($\Delta\phi$) in each of the eight cellular compartments included in Recon 1. *Variability in peroxisomal pH and $\Delta\phi$ was accounted for by adding uncertainty to standard transformed Gibbs energy estimates for peroxisomal metabolites and reactions (see Sections A.3.1 and A.3.2).

Compartment	pH	$\Delta\phi$ (mV)	References
Cytosol and nucleus	7.20	0	(4)
Extracellular fluid	7.40	30	(7, 21, 22)
Golgi apparatus	6.35	0	(6, 25, 26)
Lysosomes	5.50	19	(6, 28)
Mitochondria	8.00	-155	(69, 20)
Endoplasmic reticulum	7.20	0	(6, 26)
Peroxisomes*	7.00 ± 1.2	12 ± 74	(11, 12, 13, 14, 15), (16, 18)

Table S2: Compartment-specific concentrations for the most highly connected metabolites in Recon 1 were assembled from HMDB and literature. Metabolite names corresponding to the abbreviations in the table are given in the Supporing Data.

Metabolite	x_{min} (M)	x_{max} (M)
adp[c]	1.00×10^{-7}	1.90×10^{-3}
adp[m]	2.60×10^{-3}	9.40×10^{-3}
amp[c]	1.00×10^{-7}	1.20×10^{-3}
atp[c]	1.29×10^{-3}	4.90×10^{-3}
atp[m]	2.80×10^{-3}	2.04×10^{-2}
coa[c]	2.92×10^{-5}	1.17×10^{-4}
coa[m]	2.20×10^{-3}	3.90×10^{-3}
na1[c]	1.00×10^{-7}	2.50×10^{-2}
na1[e]	1.33×10^{-1}	1.55×10^{-1}
nad[c]	1.05×10^{-4}	7.57×10^{-4}
nad[m]	5.00×10^{-4}	7.50×10^{-3}
nadh[c]	9.26×10^{-7}	3.83×10^{-4}
nadh[m]	1.00×10^{-7}	1.10×10^{-3}
nadp[c]	1.00×10^{-7}	5.83×10^{-6}
nadp[m]	1.00×10^{-7}	1.50×10^{-3}
nadph[c]	1.00×10^{-7}	3.75×10^{-4}
nadph[m]	1.00×10^{-7}	4.20×10^{-3}
nh4[c]	7.00×10^{-4}	9.00×10^{-4}
pi[c]	1.00×10^{-3}	6.30×10^{-3}
ppi[c]	2.10×10^{-3}	7.60×10^{-3}
udp[g]	1.40×10^{-6}	1.40×10^{-4}
h2o	1.00×10^{1}	1.00×10^{1}
co2	1.00×10^{-4}	1.00×10^{-4}
co2[c]	1.00×10^{-7}	1.40×10^{-4}
o2	8.20×10^{-8}	8.20×10^{-6}
o2[c]	1.00×10^{-7}	8.20×10^{-6}
h	$1.00 \times 10^{-\mathrm{pH}}$	$1.00 \times 10^{-\mathrm{pH}}$
References	(70, 71, 72, 73, 74, 75, 76, 77)	

Table S3: Standard Gibbs energies of formation ($\Delta_f G_j^0$) for phosphate species of interest in the pH range 5-9. *Output from the group contribution method. Predominant species at pH 7.

Species	$\Delta_f G^0_{j,obs}$ (kJ/mol)	$\Delta_f G^0_{j,est}$ (kJ/mol)
HPO_4^{2-}	-1096.1	-1096.1*
$H_2PO_4^{1-}$	-1137.3	-1135.7
pK_a	7.22	6.95

A.8 Supplementary Figures

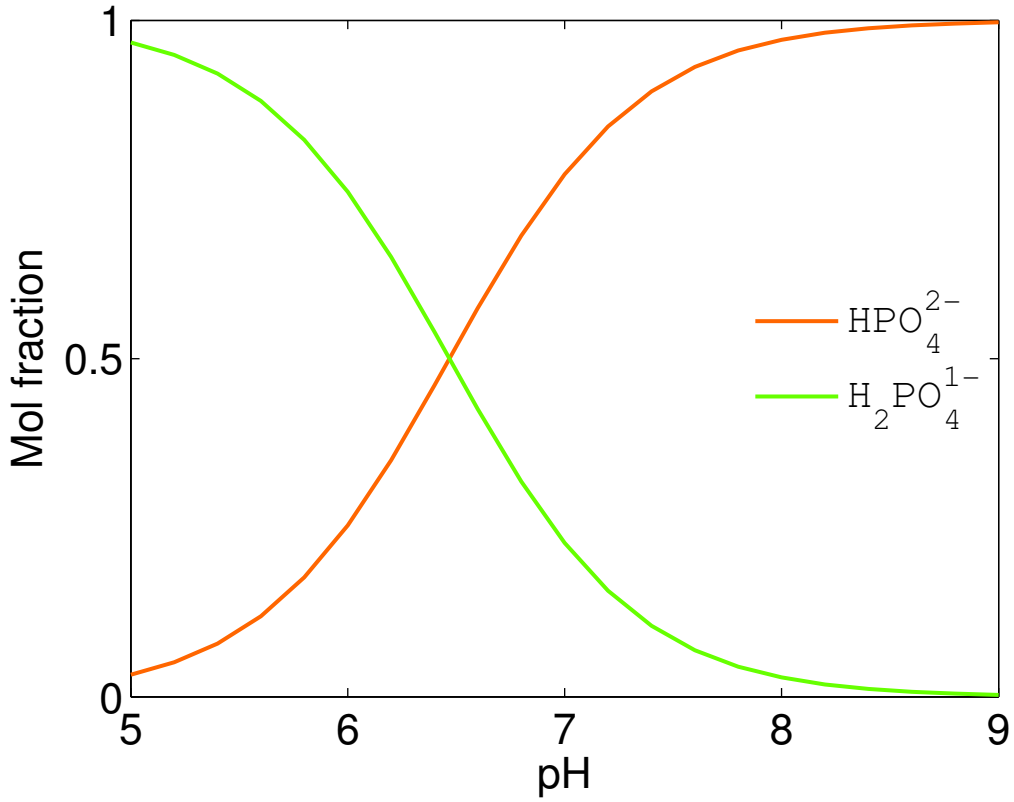

Figure S1: Species distribution for phosphate at pH 5-9, 310.15 K and 0.15 M ionic strength. Each line represents the pH-dependent relative abundance of a particular ion, or species, of phosphate.

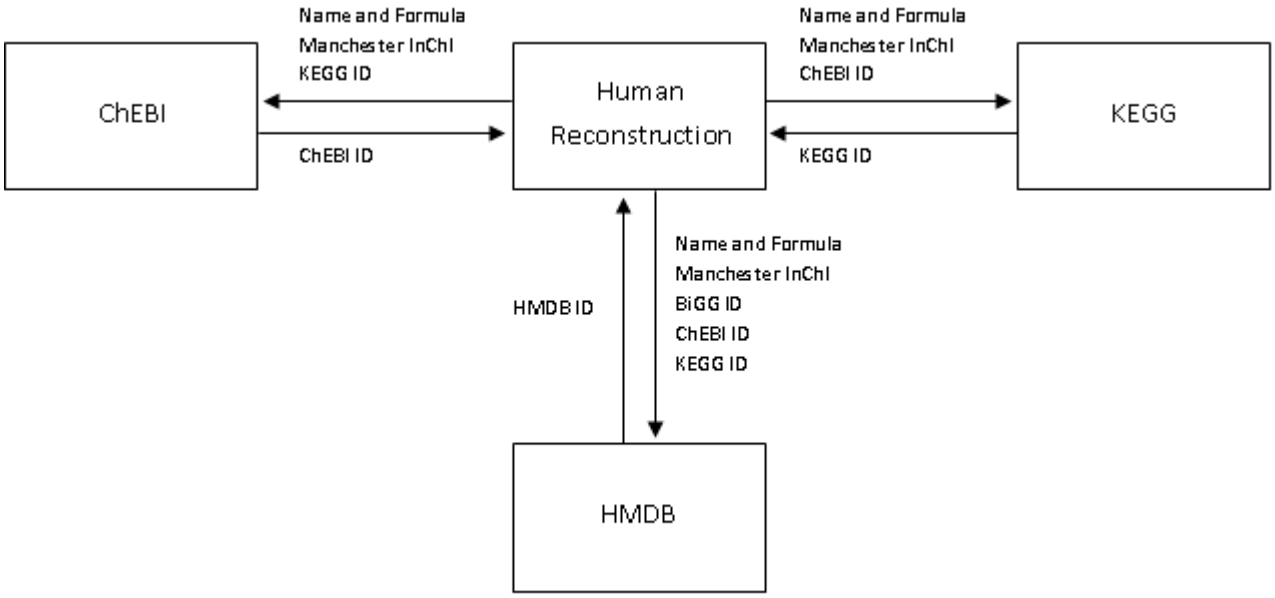

Figure S2: Schema for automatic retrieval of IUPAC International Chemical Identifiers (InChIs) from the internet databases HMDB, KEGG and ChEBI. First, metabolite data in Recon 1 was used to retrieve database specific identifiers. The database identifiers were then used to retrieve InChIs.

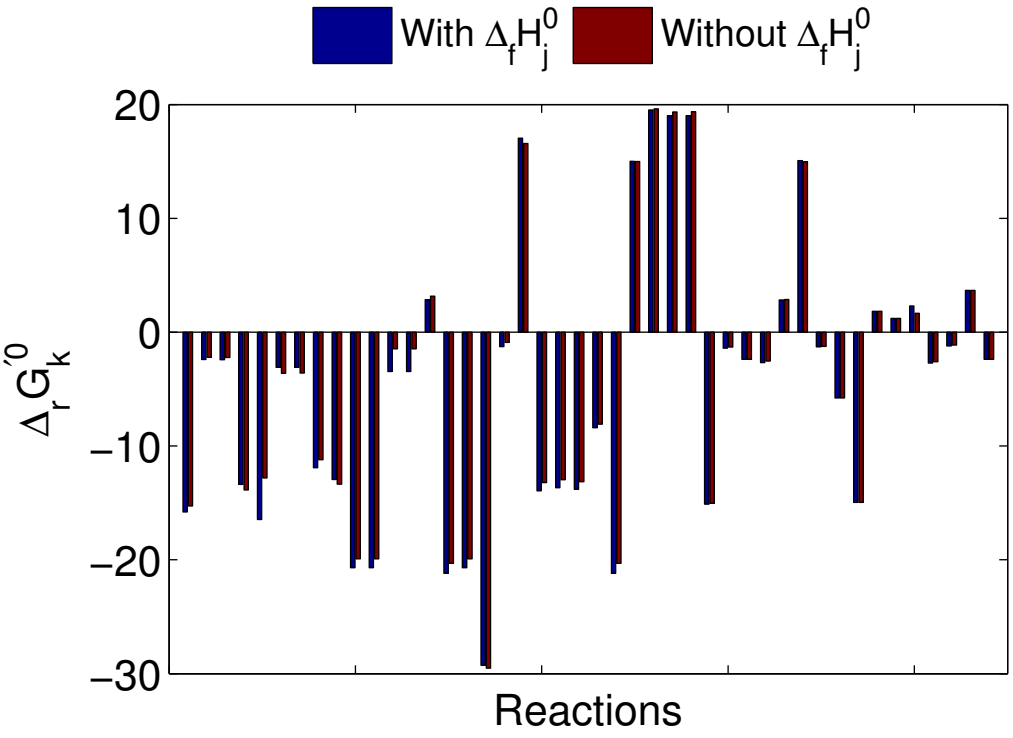

Figure S3: Standard transformed reaction Gibbs energies ($\Delta_r G'^0_k$) calculated with (*blue*) and without (*red*) data on metabolite species standard enthalpies of formation ($\Delta_f H^0_j$). The difference between the two is a measure of the contribution of entropy to $\Delta_r G'^0_k$. The entropic contribution was small for 150 reactions involving only metabolites with known $\Delta_f H^0_j$. For clarity, only those reactions that had $\Delta_r G'^0_k$ magnitudes between 1 and 50 kJ/mol are shown.

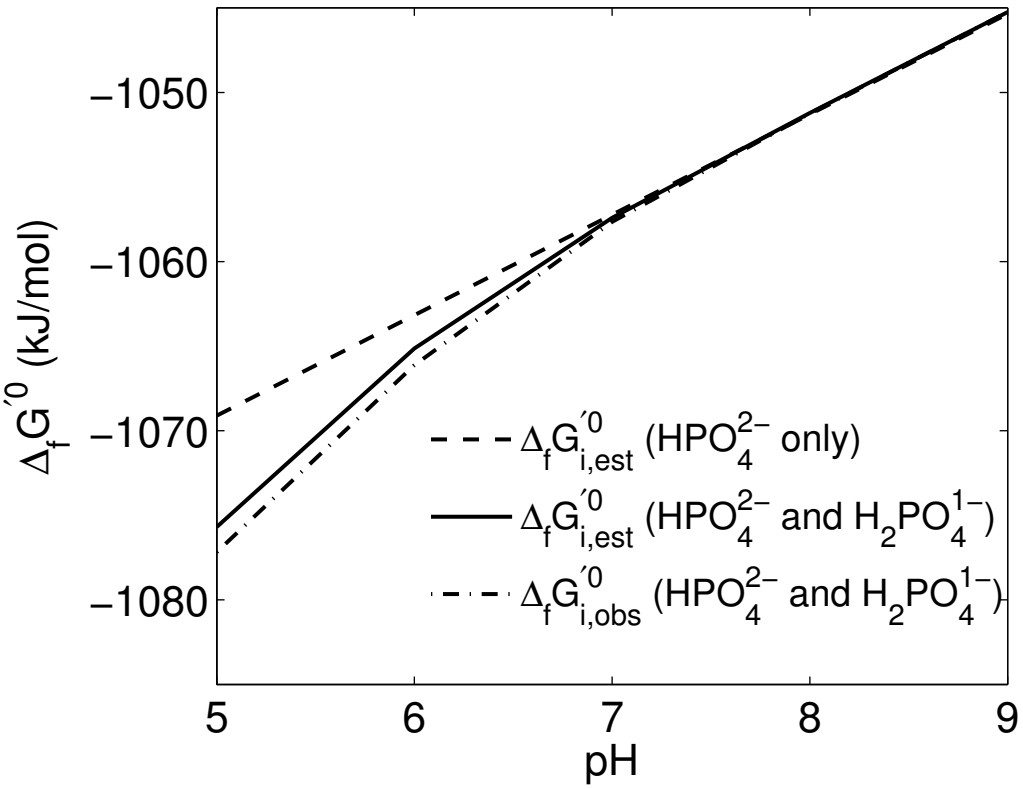

Figure S4: $\Delta_f G'^0_i$ for phosphate in the pH range 5-9. The group contribution method returned $\Delta_f G^0_{j,est}$ for HPO_4^{2-}; the predominant species at 298 K, 0 M ionic strength and pH 7. Instead of approximating $\Delta_f G'^0_{i,est}$ for phosphate at physiological conditions with $\Delta_f G'^0_{j,est}$ for HPO_4^{2-} only (*dashed straight line*), we computed $\Delta_f G^0_{j,est}$ for $H_2PO_4^{1-}$ and included it in our calculations of $\Delta_f G'^0_{i,est}$ (*solid curve*). Doing this reduced the deviation of $\Delta_f G'^0_{i,est}$ from $\Delta_f G'^0_{i,obs}$ (*dash-dot curve*) at lower pH where $H_2PO_4^{1-}$ replaces HPO_4^{2-} as the predominant species. At 310.15 K and 0.15 M ionic strength, $H_2PO_4^{1-}$ is the predominant species at all pH below 6.5. Below pH 6.5, the deviation of $\Delta_f G'^0_{i,est}$ (HPO_4^{2-} only) from $\Delta_r G'^0_{i,obs}$ decreases with pH. In contrast, $\Delta_f G'^0_{i,est}$ (HPO_4^{2-} and $H_2PO_4^{1-}$) deviates only slightly from from $\Delta_r G'^0_{i,obs}$, even at low pH.

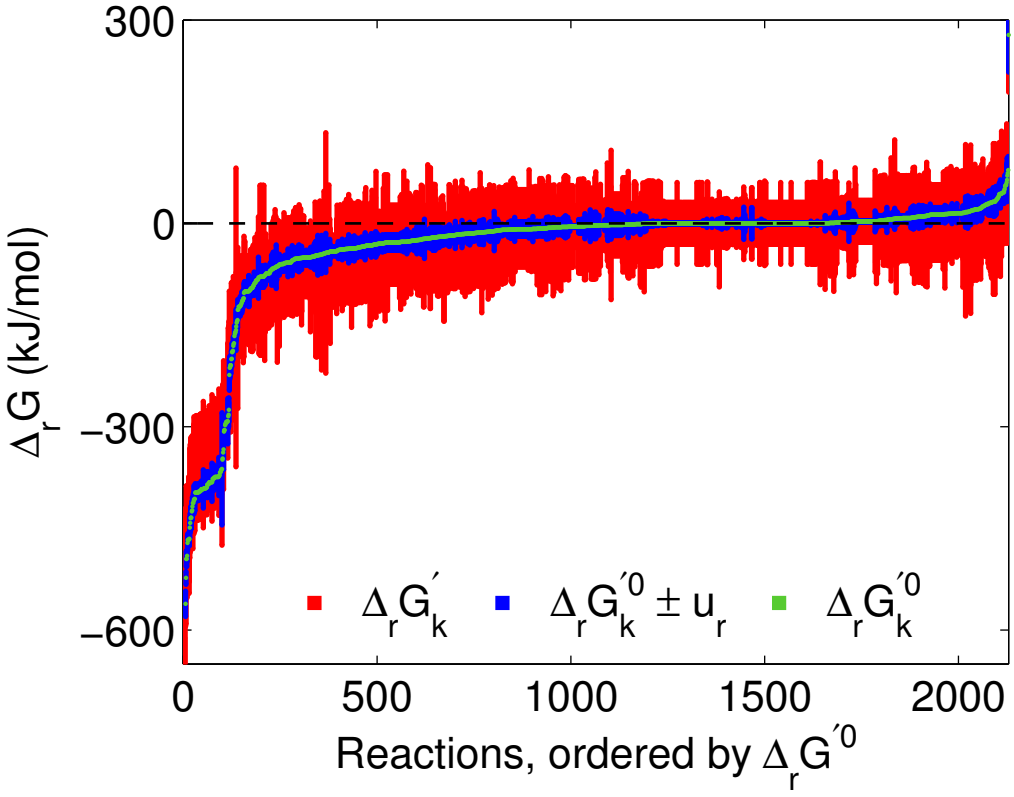

Figure S5: $\Delta_r G'^0_k \pm u_r$ for reactions in Recon 1, as well as ranges of $\Delta_r G'_k$ achievable within the specified bounds on metabolite concentrations. Reactions are sorted by increasing $\Delta_r G'^0_k$. Reactions were said to be quantitatively forward if $\Delta_r G'_{k,max} < 0$ (*leftmost reactions*), quantitatively reverse if $\Delta_r G'_{k,min} > 0$ (*rightmost reactions*), and quantitatively reversible if $\Delta_r G'_{k,min} < 0$ and $0 < \Delta_r G'_{k,max}$ (*central reactions*).

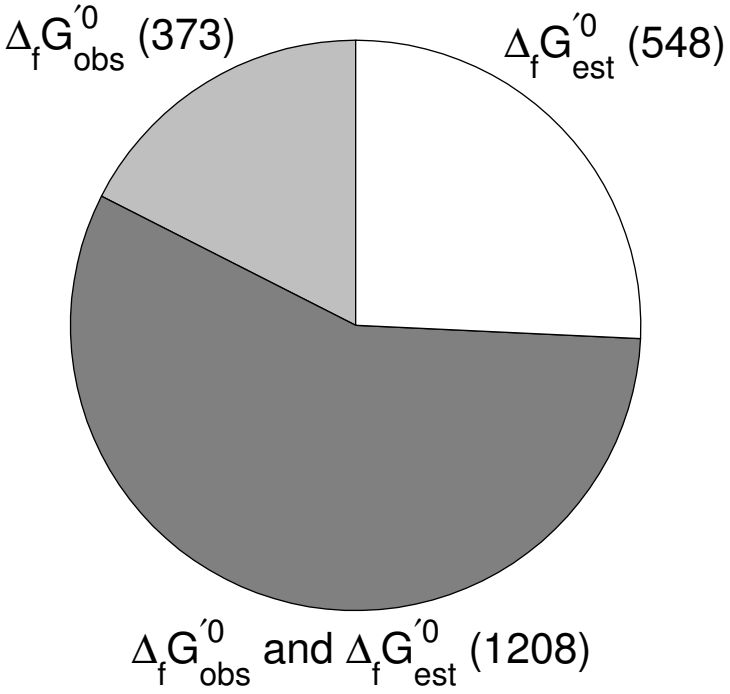

Figure S6: Number of $\Delta_r G'^0_k$ calculated from each source of $\Delta_f G'^0_i$. The majority of $\Delta_r G'^0_k$ were calculated using at least one $\Delta_f G'^0_{i,est}$.

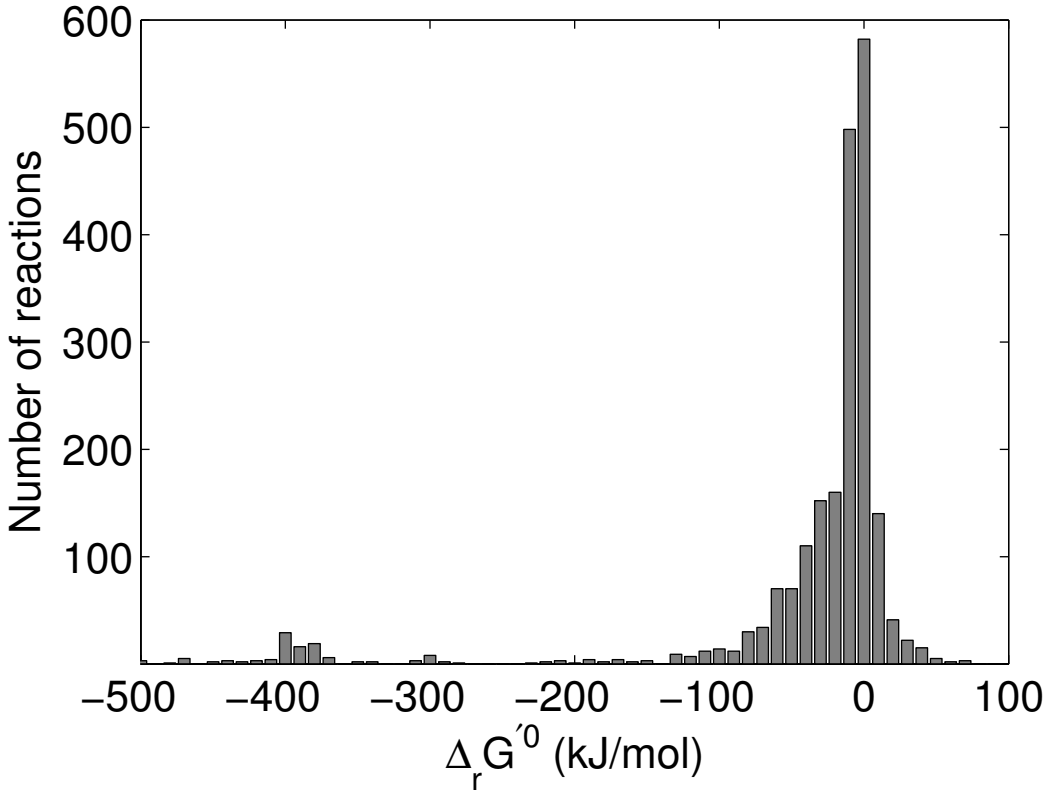

Figure S7: Distribution of $\Delta_r G'^0_k$ for 2129 reactions in Recon 1. Most reactions had $\Delta_r G'^0_k$ between -100 and 50 kJ/mol, but redox reactions involving oxygen, hydrogen peroxide, NADH or NADPH often had a much larger negative $\Delta_r G'^0_k$ of around -400 kJ/mol.

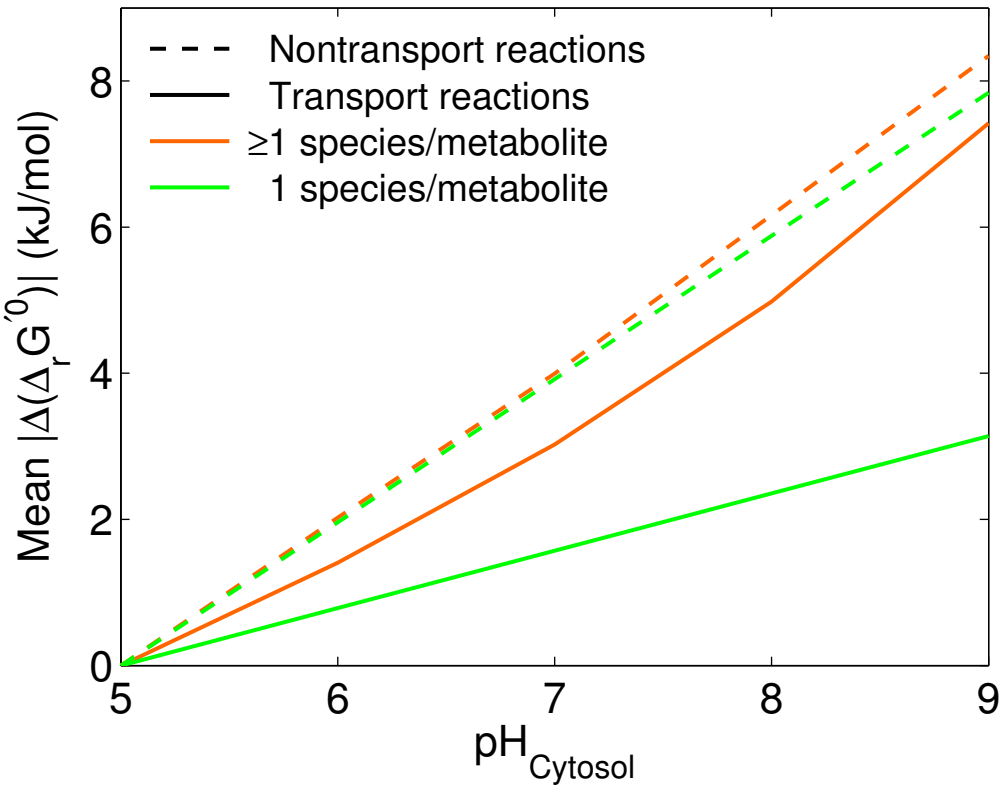

Figure S8: The effect of pH on $\Delta_r G'^0_k$ for cytosolic nontransport reactions (*dashed lines*) and all transport reactions (*solid lines*) when metabolites are represented by pseudoisomer groups of multiple ionic species (*orange lines*), and when they are represented by the single most predominant species at pH 7 (*green lines*). The figure shows changes in $\Delta_r G'^0_k$ magnitude, as cytosolic pH is varied from 5 to 9 while the pH of all other compartments is kept constant at pH 7. Representing metabolites as pseudoisomer groups is particularly important for transport reactions.

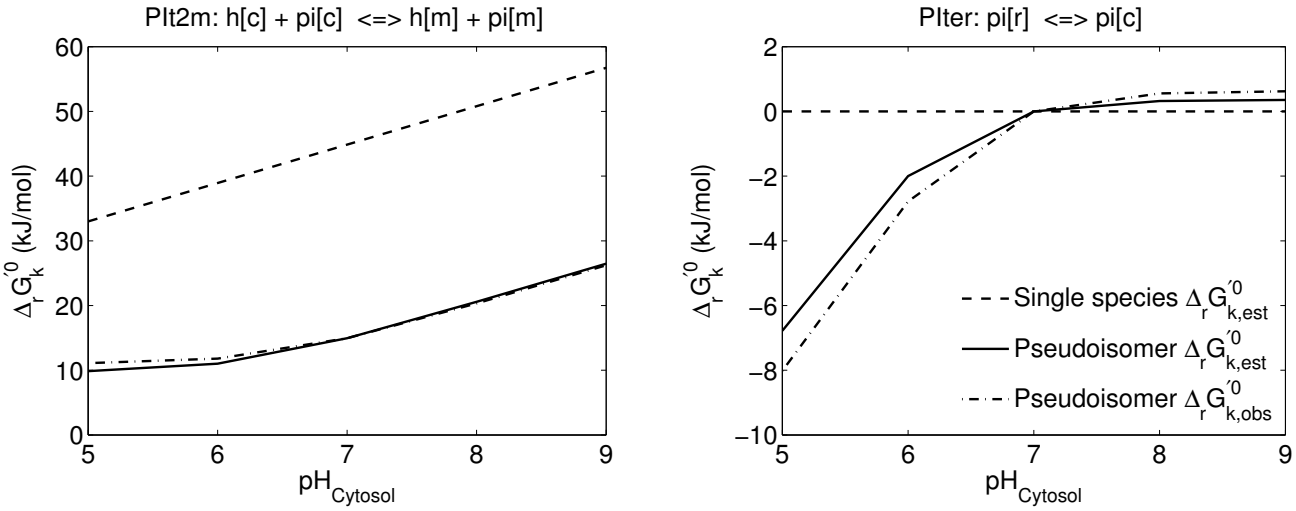

(a) (b)

Figure S9: The effect of compartmental differences in pH on $\Delta_r G'^0_k$ for transport reactions involving phosphate. Cytosolic pH was increased from 5 to 9 while the pH of the second compartment was kept constant at pH 7. (a) Increasing cytosolic pH affects $\Delta_r G'^0_{k,obs}$ (*dash-dot curve*) for proton-phosphate symport into the mitochondria by altering the distribution of phosphate species and the chemical potential of the proton. Both effects are captured in $\Delta_r G'^0_{k,est}$ when phosphate is represented as a pseudoisomer group consisting of both HPO_4^{2-} and $H_2PO_4^{1-}$ (*solid curve*). When phosphate is represented by HPO_4^{2-} only, variations in cytosolic pH still affect the chemical potential of the proton but not the distribution of phosphate species. This leads to large errors in $\Delta_r G'^0_{k,est}$ (*dashed line*). (b) $\Delta_r G'^0_{k,est}$ for passive diffusion of phosphate between the ER and cytosol is not affected by variations in cytosolic pH when phosphate is represented by HPO_4^{2-} only, because no protons are transported.

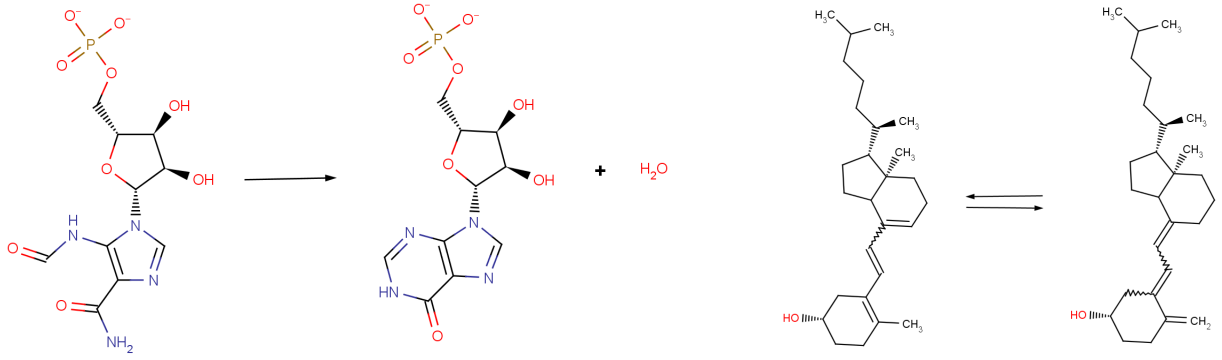

(a) (b)

Figure S10: The group contribution method appears unsuitable for estimation of reaction Gibbs energies for complex structural transformations such as (a) the closing of the pyrimidine ring in IMP and (b) the translocation of double bonds in vitamin D3. Reaction diagrams were created in MarvinSketch (v5.3.7, ChemAxon, Budapest, Hungary).

SUPPLEMENTARY REFERENCES

1. Bevensee, M. O., and W. F. Boron, 2008. Control of intracellular pH. *In* R. J. Alpern, and S. C. Hebert, editors, Seldin and Giebisch's the kidney, Academic Press, Burlington, MA, 1429–1480.

2. Lin, H. J., P. Herman, and J. R. Lakowicz, 2003. Fluorescence lifetime-resolved pH imaging of living cells. *Cytometry, Part A* 52:77–89.

3. Eisner, D. A., N. A. Kenning, S. C. O'Neill, G. Pocock, C. D. Richards, and M. Valdeolmillos, 1989. A novel method for absolute calibration of intracellular pH indicators. *Pflügers Arch.* 413:553–558.

4. Buckler, K. J., and R. D. Vaughan-Jones, 1990. Application of a new pH-sensitive fluoroprobe (carboxy-SNARF-1) for intracellular pH measurement in small, isolated cells. *Pflügers Arch.* 417:234–239.

5. Benink, H., M. McDougall, D. Klaubert, and G. Los, 2009. Direct pH measurements by using subcellular targeting of 5(and 6-) carboxyseminaphthorhodafluor in mammalian cells. *BioTechniques* 47:769–774.

6. Paroutis, P., N. Touret, and S. Grinstein, 2004. The pH of the secretory pathway: measurement, determinants, and regulation. *Physiology* 19:207–215.

7. Street, D., J. Bangsbo, and C. Juel, 2001. Interstitial pH in human skeletal muscle during and after dynamic graded exercise. *J. Physiol.* 537:993–998.

8. Abad, M. F. C., G. Di Benedetto, P. J. Magalhaes, L. Filippin, and T. Pozzan, 2004. Mitochondrial pH monitored by a new engineered green fluorescent protein mutant. *J. Biol. Chem.* 279:11521–11529.

9. Llopis, J., J. M. McCaffery, A. Miyawaki, M. G. Farquhar, and R. Y. Tsien, 1998. Measurement of cytosolic, mitochondrial, and Golgi pH in single living cells with green fluorescent proteins. *Proc Natl Acad Sci USA* 95:6803–6808.

10. Porcelli, A. M., A. Ghelli, C. Zanna, P. Pinton, R. Rizzuto, and M. Rugolo, 2005. pH difference across the outer mitochondrial membrane measured with a green fluorescent protein mutant. *Biochem. Biophys. Res. Commun.* 326:799–804.

11. Dansen, T. B., K. W. A. Wirtz, R. J. A. Wanders, and E. H. W. Pap, 1999. Peroxisomes in human fibroblasts have a basic pH. *Nat. Cell. Biol.* 2:51–53.

12. Douma, A. C., M. Veenhuis, G. J. Sulter, and W. Harder, 1987. A proton-translocating adenosine triphosphatase is associated with the peroxisomal membrane of yeasts. *Arch. Microbiol.* 147:42–47.

13. Jankowski, A., J. H. Kim, R. F. Collins, R. Daneman, P. Walton, and S. Grinstein, 2001. In situ measurements of the pH of mammalian peroxisomes using the fluorescent protein pHluorin. *J. Biol. Chem.* 276:48748–48753.

14. Nicolay, K., M. Veenhuis, A. C. Douma, and W. Harder, 1987. A 31 P NMR study of the internal pH of yeast peroxisomes. *Arch. Microbiol.* 147:37–41.

15. van Roermund, C. W. T., M. de Jong, L. IJlst, J. van Marle, T. B. Dansen, R. J. A. Wanders, and H. R. Waterham, 2004. The peroxisomal lumen in *Saccharomyces cerevisiae* is alkaline. *J. Cell. Sci.* 117:4231–4237.

16. Antonenkov, V. D., and J. K. Hiltunen, 2006. Peroxisomal membrane permeability and solute transfer. *Biochim. Biophys. Acta, Mol. Cell. Res.* 1763:1697–1706.

17. Antonenkov, V. D., R. T. Sormunen, and J. K. Hiltunen, 2004. The rat liver peroxisomal membrane forms a permeability barrier for cofactors but not for small metabolites in vitro. *J. Cell. Sci.* 117:5633–5642.

18. Antonenkov, V. D., and J. K. Hiltunen, 2011. Transfer of metabolites across the peroxisomal membrane. *Biochim. Biophys. Acta* .

19. Huttemann, M., I. Lee, A. Pecinova, P. Pecina, K. Przyklenk, and J. W. Doan, 2008. Regulation of oxidative phosphorylation, the mitochondrial membrane potential, and their role in human disease. *J. Bioenerg. Biomembr.* 40:445–456.

20. Cortese, J. D., 1999. Rat liver GTP-binding proteins mediate changes in mitochondrial membrane potential and organelle fusion. *Am. J. Physiol.* 276:C611–C620.

21. Hoek, J. B., D. G. Nicholls, and J. R. Williamson, 1980. Determination of the mitochondrial protonmotive force in isolated hepatocytes. *J. Biol. Chem.* 255:1458–1464.

22. Nobes, C. D., G. C. Brown, P. N. Olive, and M. D. Brand, 1990. Non-ohmic proton conductance of the mitochondrial inner membrane in hepatocytes. *J. Biol. Chem.* 265:12903–12909.

23. Williams, J. A., 1970. Origin of transmembrane potentials in non-excitable cells. *J. Theor. Biol.* 28:287–296.

24. Glickman, J., K. Croen, S. Kelly, and Q. Al-Awqati, 1983. Golgi membranes contain an electrogenic H+ pump in parallel to a chloride conductance. *J. Cell. Biol.* 97:1303–1308.

25. Schapiro, F. B., and S. Grinstein, 2000. Determinants of the pH of the Golgi complex. *J. Biol. Chem.* 275:21025–21032.

26. Wu, M. M., J. Llopis, S. Adams, J. M. McCaffery, M. S. Kulomaa, T. E. Machen, H. P. Moore, and R. Y. Tsien, 2000. Organelle pH studies using targeted avidin and fluorescein-biotin. *Chem. Biol.* 7:197–209.

27. Kim, J. H., L. Johannes, B. Goud, C. Antony, C. A. Lingwood, R. Daneman, and S. Grinstein, 1998. Noninvasive measurement of the pH of the endoplasmic reticulum at rest and during calcium release. *Proc. Natl. Acad. Sci. U. S. A.* 95:2997–3002.

28. Koivusalo, M., B. E. Steinberg, D. Mason, and S. Grinstein, 2011. In situ measurement of the electrical potential across the lysosomal membrane using FRET. *Traffic* 12:972–982.

29. Jankowski, M. D., C. S. Henry, L. J. Broadbelt, and V. Hatzimanikatis, 2008. Group contribution method for thermodynamic analysis of complex metabolic networks. *Biophys. J.* 95:1487–1499.

30. Szegezdi, J., and F. Csizmadia. A method for calculating the pKa values of small and large molecules. American Chemical Society Spring meeting; Chicago, IL, 2007.

31. Alberty, R. A., 2003. Thermodynamics of Biochemical Reactions. Wiley-Interscience, Hoboken, NJ.

32. Alberty, R. A., 1997. Legendre transforms in chemical thermodynamics. *J. Chem. Thermodyn.* 29:501–516.

33. Alberty, R. A., 2006. Biochemical Thermodynamics: Applications of Mathematica. Wiley-Interscience, Hoboken, NJ.

34. Jol, S., A. Kümmel, V. Hatzimanikatis, D. Beard, and M. Heinemann, 2010. Thermodynamic Calculations for Biochemical Transport and Reaction Processes in Metabolic Networks. *Biophys. J.* 99:3139–3144.

35. Planck, M., 1993. A Survey of Physical Theory. Courier Dover Publications, Chelmsford, MA.

36. Dill, K. A., and S. Bromberg, 2003. Molecular driving forces: Statistical thermodynamics in Chemistry and Biology. Garland Science, London.

37. Callen, H. B., 1985. Thermodynamics and an Introduction to Thermostatistics. John Wiley & Sons, New York.

38. Thiele, I., N. Jamshidi, R. M. T. Fleming, and B. Ø. Palsson, 2009. Genome-scale reconstruction of *E. coli*'s transcriptional and translational machinery: a knowledge-base, its mathematical formulation, and its functional characterization. *PLoS Comput. Biol.* 5:e1000312.

39. Yang, F., H. Qian, and D. A. Beard, 2005. Ab initio prediction of thermodynamically feasible reaction directions from biochemical network stoichiometry. *Metab. Eng.* 7:251–259.

40. Gibbs, J. W., 1902. Elementary principles in statistical mechanics, developed with especial reference to the rational foundation of thermodynamics. Dover Publications, New York.

41. Alberty, R. A., 2003. Standard transformed Gibbs energies of coenzyme A derivatives as functions of pH and ionic strength. *Biophys. Chem.* 104:327–334.

42. Alberty, R. A., 2003. The role of water in the thermodynamics of dilute aqueous solutions. *Biophys. Chem.* 100:183–192.

43. Henry, C. S., L. J. Broadbelt, and V. Hatzimanikatis, 2007. Thermodynamics-based metabolic flux analysis. *Biophys. J.* 92:1792–1805.

44. Bulock, K. G., G. P. Beardsley, and K. S. Anderson, 2002. The kinetic mechanism of the human bifunctional enzyme ATIC (5-amino-4-imidazolecarboxamide ribonucleotide transformylase/inosine 5'-monophosphate cyclohydrolase). A surprising lack of substrate channeling. *J. Biol. Chem.* 277:22168–22174.

45. Holick, M. F., J. A. MacLaughlin, M. B. Clark, S. A. Holick, J. T. Potts Jr, R. R. Anderson, I. H. Blank, J. A. Parrish, and P. Elias, 1980. Photosynthesis of previtamin D3 in human skin and the physiologic consequences. *Science* 210:203–205.

46. Tian, X. Q., and M. F. Holick, 1995. Catalyzed thermal isomerization between previtamin D and vitamin D via cyclodextrin complexation. *J. Biol. Chem.* 270:8706–8711.

47. Schmid, R., 1972. Bilirubin metabolism in man. *N. Engl. J. Med.* 287:703–709.

48. Belinsky, M. G., P. A. Dawson, I. Shchaveleva, L. J. Bain, R. Wang, V. Ling, Z.-S. Chen, A. Grinberg, H. Westphal, A. Klein-Szanto, A. Lerro, and G. D. Kruh, 2005. Analysis of the in vivo functions of Mrp3. *Mol. Pharmacol.* 68:160–168.

49. Kanehisa, M., S. Goto, M. Furumichi, M. Tanabe, and M. Hirakawa, 2010. KEGG for representation and analysis of molecular networks involving diseases and drugs. *Nucleic Acids Res.* 38:D355–D360.

50. Forte-McRobbie, C. M., and R. Pietruszko, 1986. Purification and characterization of human liver "high Km" aldehyde dehydrogenase and its identification as glutamic gamma-semialdehyde dehydrogenase. *J. Biol. Chem.* 261:2154–2163.

51. Hu, C. A., W. W. Lin, and D. Valle, 1996. Cloning, characterization, and expression of cDNAs encoding human delta 1-pyrroline-5-carboxylate dehydrogenase. *J. Biol. Chem.* 271:9795–9800.

52. Uotila, L., and M. Koivusalo, 1974. Formaldehyde dehydrogenase from human liver. Purification, properties, and evidence for the formation of glutathione thiol esters by the enzyme. *J. Biol. Chem.* 249:7653–7663.

53. Uotila, L., and M. Koivusalo, 1974. Purification and properties of S-formylglutathione hydrolase from human liver. *J. Biol. Chem.* 249:7664–7672.

54. Wu, G., Y. Z. Fang, S. Yang, J. R. Lupton, and N. D. Turner, 2004. Glutathione metabolism and its implications for health. *J. Nutr.* 134:489–492.

55. Schafer, F. Q., and G. R. Buettner, 2001. Redox environment of the cell as viewed through the redox state of the glutathione disulfide/glutathione couple. *Free Radic. Biol. Med.* 30:1191–1212.

56. Wada, H., and E. E. Snell, 1961. The enzymatic oxidation of pyridoxine and pyridoxamine phosphates. *J. Biol. Chem.* 236:2089–2095.

57. McCormick, D. B., and H. Chen, 1999. Update on interconversions of vitamin B-6 with its coenzyme. *J. Nutr.* 129:325–327.

58. Fitzpatrick, T., N. Amrhein, B. Kappes, P. Macheroux, I. Tews, and T. Raschle, 2007. Two independent routes of *de novo* vitamin B6 biosynthesis: not that different after all. *Biochem. J.* 407:1–13.

59. Crabbe, M. J., R. D. Waight, W. G. Bardsley, R. W. Barker, I. D. Kelly, and P. F. Knowles, 1976. Human placental diamine oxidase. Improved purification and characterization of a copper- and manganese-containing amine oxidase with novel substrate specificity. *Biochem. J.* 155:679–687.

60. Blaner, W. S., 2001. Cellular metabolism and actions of 13-cis-retinoic acid. *J. Am. Acad. Dermatol.* 45:S129–S135.

61. Moffa, D. J., F. J. Lotspeich, and R. F. Krause, 1970. Preparation and properties of retinal-oxidizing enzyme from rat intestinal mucosa. *J. Biol. Chem.* 245:439–447.

62. Leonardi, R., Y. Zhang, C. O. Rock, and S. Jackowski, 2005. Coenzyme A: back in action. *Prog. Lipid Res.* 44:125–153.

63. Fiermonte, G., E. Paradies, S. Todisco, C. M. T. Marobbio, and F. Palmieri, 2009. A novel member of solute carrier family 25 (SLC25A42) is a transporter of coenzyme A and adenosine 3',5'-diphosphate in human mitochondria. *J. Biol. Chem.* 284:18152–18159.

64. Venkatachalam, K. V., 2003. Human 3'-phosphoadenosine 5'-phosphosulfate (PAPS) synthase: biochemistry, molecular biology and genetic deficiency. *IUBMB Life* 55:1–11.

65. Robbins, P. W., and F. Lipmann, 1958. Enzymatic synthesis of adenosine-5'-phosphosulfate. *J. Biol. Chem.* 233:686–690.

66. Akagi, J. M., and L. L. Campbell, 1962. STUDIES ON THERMOPHILIC SULFATE-REDUCING BACTERIA III. : Adenosine Triphosphate-sulfurylase of Clostridium nigrificans and Desulfovibrio desulfuricans. *J. Bacteriol.* 84:1194–1201.

67. Wilson, L. G., and R. S. Bandurski, 1958. Enzymatic reactions involving sulfate, sulfite, selenate, and molybdate. *J. Biol. Chem.* 233:975–981.

68. Farley, J. R., D. F. Cryns, Y. H. Yang, and I. H. Segel, 1976. Adenosine triphosphate sulfurylase from penicillium chrysogenum. Steady state kinetics of the forward and reverse reactions. *J. Biol. Chem.* 251:4389–4397.

69. Llopis, J., J. M. McCaffery, A. Miyawaki, M. G. Farquhar, and R. Y. Tsien, 1998. Measurement of cytosolic, mitochondrial, and Golgi pH in single living cells with green fluorescent proteins. *Proc Natl Acad Sci USA* 95:6803–6808.

70. Wishart, D. S., C. Knox, A. C. Guo, R. Eisner, N. Young, B. Gautam, D. D. Hau, N. Psychogios, E. Dong, S. Bouatra, R. Mandal, I. Sinelnikov, J. Xia, L. Jia, J. A. Cruz, E. Lim, C. A. Sobsey, S. Shrivastava, P. Huang, P. Liu, L. Fang, J. Peng, R. Fradette, D. Cheng, D. Tzur, M. Clements, A. Lewis, A. D. Souza, A. Zuniga, M. Dawe, Y. Xiong, D. Clive, R. Greiner, A. Nazyrova, R. Shaykhutdinov, L. Li, H. J. Vogel, and I. Forsythe, 2009. HMDB: a knowledgebase for the human metabolome. *Nucleic Acids Res.* 37:D603–D610.

71. Traut, T. W., 1994. Physiological concentrations of purines and pyrimidines. *Mol. Cell. Biochem.* 140:1–22.

72. Guynn, R. W., D. Veloso, J. W. R. Lawson, and R. L. Veech, 1974. The concentration and control of cytoplasmic free inorganic pyrophosphate in rat liver in vivo. *Biochem. J.* 140:369–375.

73. Frank, A., U. Rauen, and H. de Groot, 2000. Protection by glycine against hypoxic injury of rat hepatocytes: inhibition of ion fluxes through nonspecific leaks. *J. Hepatol.* 32:58–66.

74. Baartscheer, A., C. A. Schumacher, and J. W. Fiolet, 1997. Small changes of cytosolic sodium in rat ventricular myocytes measured with SBFI in emission ratio mode. *J. Mol. Cell. Cardiol.* 29:3375–3383.

75. Kuhn, N. J., and A. White, 1977. The role of nucleoside diphosphatase in a uridine nucleotide cycle associated with lactose synthesis in rat mammary-gland Golgi apparatus. *Biochem. J.* 168:423–433.

76. Siess, E. A., D. G. Brocks, H. K. Lattke, and O. H. Wieland, 1977. Effect of glucagon on metabolite compartmentation in isolated rat liver cells during gluconeogenesis from lactate. *Biochem. J.* 166:225–235.

77. Tischler, M. E., D. Friedrichs, K. Coll, and J. R. Williamson, 1977. Pyridine nucleotide distributions and enzyme mass action ratios in hepatocytes from fed and starved rats. *Arch. Biochem. Biophys.* 184:222–236.